Fermilab

Fermi National Accelerator Laboratory
P.O. Box 500 • Batavia, Illinois • 60510

TD – 01 – 064
September 5, 2001

Nb_3Sn Cos(θ) Dipole Magnet, HFDA-03 Production Report

D. R. Chichili[1], N. Andreev[1], E. Barzi[2], V.V. Kashikhin[2], I. Terechkine[1], S. Yadav[1], R. Yamada[2], and A.V. Zlobin[2]

[1]Engineering and Fabrication Department
[2]Development and Test Department
Technical Division
Fermilab, Batavia, IL 60510

1.0 INTRODUCTION

HFDA-03 is the third Nb_3Sn shell-type magnet to be fabricated and the second to be tested. The dipole model is a 1 m long magnet with 43.5 mm bore aperture. Fig. 1 shows the completed magnet ready to be tested. The magnet design is identical to HFDA-01[1]. The fabrication procedure followed is similar to that of HFDA-02[2] with some modifications especially the splicing procedure to eliminate strand damage, which we believe, was one of the main causes for the poor quench performance of HFDA-02.

Fig. 1: *Photograph of HFDA-03 ready to be shipped to VMTF.*

The specific features of HFDA-03 are listed below:

- The two half-coils of HFDA-03 have almost the same azimuthal size. Note that for HFDA-02, one half-coil was about 0.2 mm larger than the other due to difference in mid-thickness of the bare cable used. See Section –3 for details.

- Ground Insulation consisted of three layers of 0.125 mm thick ceramic cloth with the strip heaters weaved into the middle layer. Two layers of 0.25 mm thick ceramic cloth were used in HFDA-02.

- Voltage taps were installed on the outer layer of each half coil near the inner to outer transition. Thin stainless steel strips were soldered on to the cable after reaction.

- New splice tooling was designed and procured for this magnet. Each Nb_3Sn lead was spliced independently of the other and this enabled greater flexibility in adjusting the tooling. Further copper boxes were not used for the splice joints. See Section – 5 for details.

[1] HFDA-01 Production Report, TD-00-069
[2] HFDA-02 Production Report, TD-01-036

- The half-coil splice assembly was achieved without fixing the leads using "green putty" to the G-10 spacers. This would enable the leads to move under Lorentz forces if necessary.

- Iron yoke design was optimized for this magnet taking into account the saturation effects. Fig. 2 shows the new design.

- The stainless steel laminations were extended to cover part of the splice support block. This is to push the discontinuity in stress away from the Nb_3Sn lead.

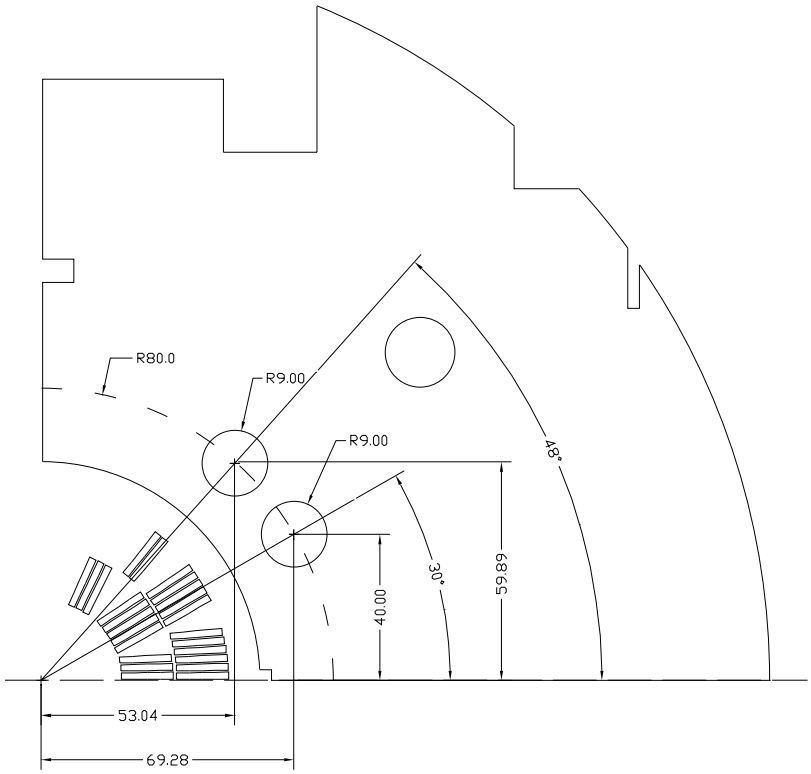

Fig. 2: *Optimized iron yoke design used in HFDA-03.*

Most of the details of the fabrication were discussed in HFDA-01 and HFDA-02 production reports. This report will summarize the data collected during production of HFDA-03.

2.0 STRAND and CABLE

The conductor used for HFDA-03 was manufactured by OST using Modified Jelly Roll Process. The nominal diameter of the strand was 1.00 mm with an effective filament diameter of 115 μm. The Cu to non-Cu ratio was 0.92. The critical current for a virgin strand and an extracted strand which were placed as witness samples in the reaction fixture along with the coil was measured to be 723 A and 662 A respectively at 12 T. Based on these results, the magnet short sample limit is estimated to be 11 T at 20.08 kA.

There were three virgin strand and three extracted strand samples placed as witness samples in the reaction fixture. The placement of these samples are as shown in the Fig. 3. Out of the three extracted samples, two of them failed during testing. Only one sample behaved as a superconducting strand.

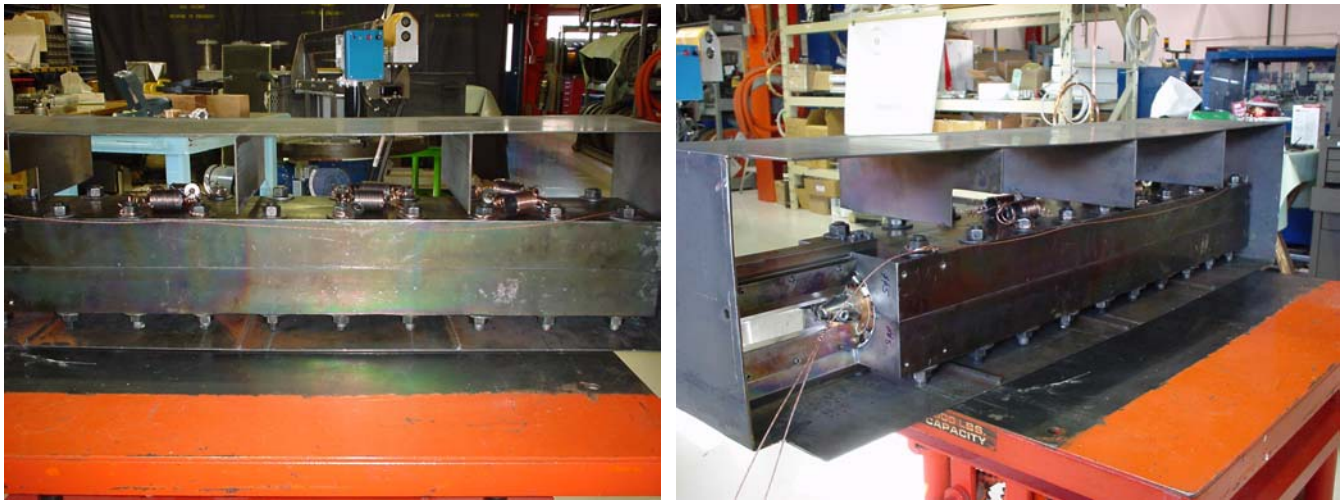

Fig. 3: *Placement of the witness samples in the retort.*

Rutherford type cable with 25 μm thick stainless steel core was manufactured at LBNL. The cable parameters are listed in Table 1. The cable was initially cleaned with ABZOL-VG to remove any oil residue left from the cabling process. It was then heat-treated at 200 ^{o}C for 30 min to reduce the residual twist in the cable that also comes from the cabling process.

Parameter	Unit	Value
Mid-Thickness	mm	1.8154
Width	mm	14.242
Keystone angle	deg	0.905
Pitch Length	mm	109.8
Number of Strands		28
Lay Direction		Left
Reel Number		782

Table 1: *Cable parameters as provided by LBNL.*

3.0 COIL FABRICATION

During the production of HFDA-02, a procedure for optimizing the coil size by varying the insulation overlap was developed so that the coil will be at the nominal size after reaction [2]. The same procedure was used for HFDA-03 coils.

3.1 Coil Winding and Curing

The two half coils were wound and cured similar to HFDA-02 coils. The only difference being the ground insulation consisted of three layers of 0.125 mm thick insulation with strip heaters weaved in the middle layer. This design was similar to that of the inter-layer insulation design in HFDA-01. Fig. 4 shows the middle layer of the ground insulation being placed on the half coil. Fig. 5 shows the heater-wiring diagram for this magnet.

Fig. 4: *Middle layer of the ground insulation with strip-heaters.*

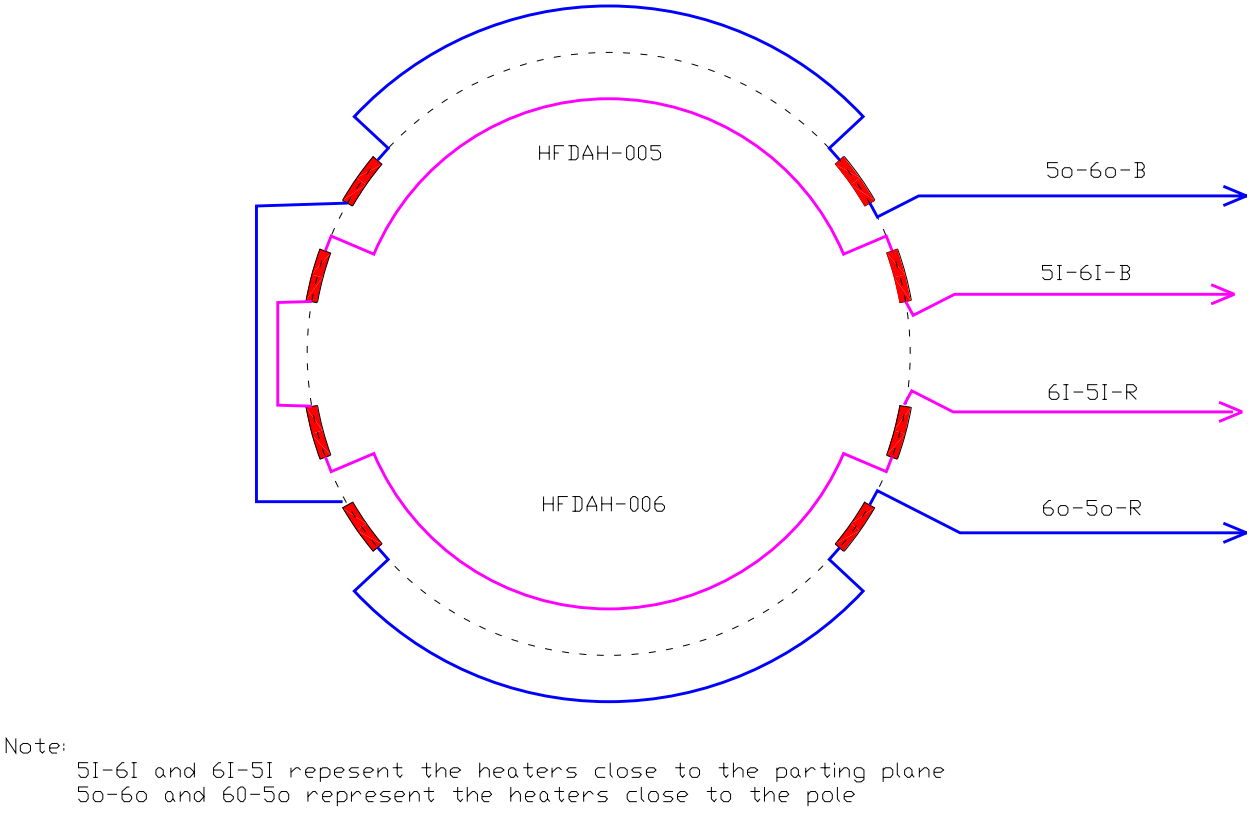

Fig. 5: *HFDA-03 heaters wiring diagram.*

3.2 Coil Electrical and Mechanical Measurements

Electrical measurements (L, Q and R) were taken on both the half coils before placing them into the reaction fixture to check for possible turn-to-turn shorts. The data is shown in Table 2. Both the coils have similar values and match the theoretical estimates, which indicate that the coils are free from turn-to-turn shorts. Note that the inductance, L and Q were measured at 1 kHz. Resistance was measured using four-wire technique at 0.1 A.

	Resistance mΩ	Inductance μH	Q
HFDAH-05	59.27	245.856	6.94
HFDAH-06	58.26	245.698	7.14

Table 2: *Electrical measurements on the cured half-coils.*

The azimuthal size in the straight section of the two half-coils was measured at two positions at varying pressures. Fig. 6 shows the data with respect to the nominal size. Note that these measurements were taken before the installation of the ground insulation. The mean azimuthal size of HFDAH-05 is 1.65 mm below the nominal size, where as HFDAH-06 is about 1.7 mm below the nominal size. The average increase in size due to reaction for a cable with insulation is about 100 μm. For a total of 13 turns, the increase will be 1.3 mm, but on an average the half coils are 1.65 mm below the nominal size. So to compensate for the size 250 μm thick ceramic tape was added at the mid-plane of the each half-coil which resulted in 0.5 mm of extra mid-plane insulation between the two half-coils.

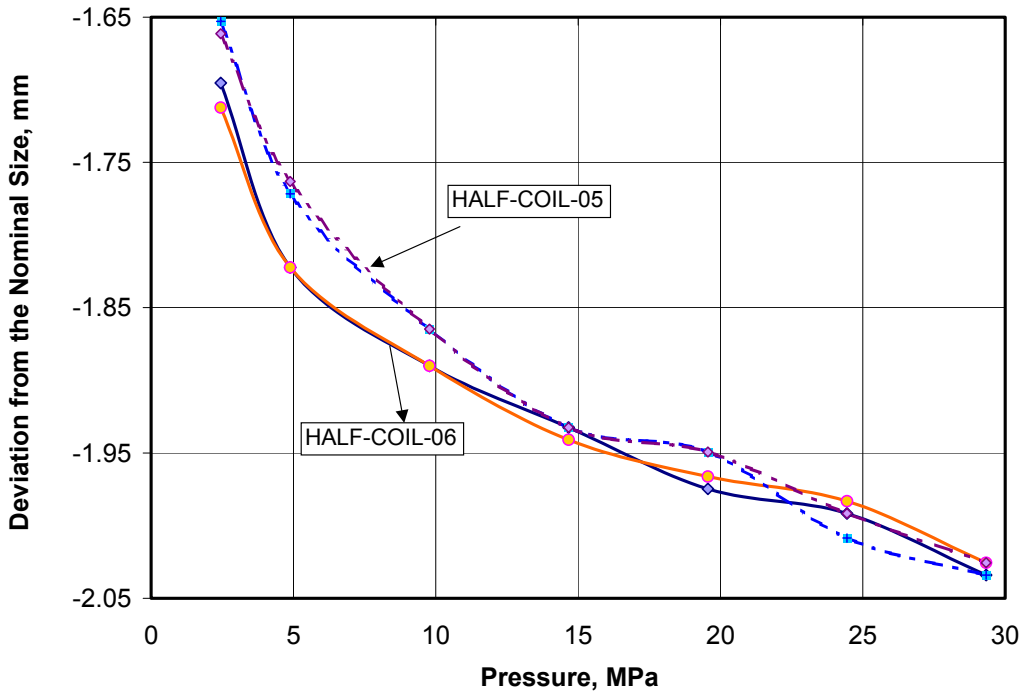

Fig. 6: *Azimuthal coil size variation with pressure at two positions along the straight section of the coil.*

4.0 COIL REACTION

The reaction cycle followed for HFDA-03 is similar to that of HFDA-02 and is given in Table 3. The two half-coils were assembled into the reaction fixture and then placed inside the retort. Since the coils were undersized, the two halves of the reaction fixture closed very easily. Two thermocouples were attached to the either end of the stainless steel mandrel to measure the temperature of coil and a third one was placed inside the retort to measure the temperature of the argon. The measured temperature profiles are shown in HFDA-02 production report [TD-01-036].

	Ramp Rate ^{o}C/hr	Temperature ^{o}C	Dwell Time hr
Step - 1	25	210	100
Step - 2	50	340	48
Step - 3	75	650	180

Table 3: *Heat-treatment cycle used in HFDA-03*.

5.0 SPLICE JOINTS

A new splice tooling was designed for this magnet. Each Nb_3Sn lead was spliced individually to two NbTi leads to avoid strand damage during the operation. The reaction fixture with the coil assembly in it was first placed on the rollers used to exchange with the impregnation fixture. The fixture was then rotated slightly so that the Nb_3Sn lead is parallel to the splicing fixture. Fig. 7 shows the set up. Once the leads are placed into the assembly, it was spring loaded before heating. The tooling was made flexible to account for any motion during the heating process. Fig. 7(a) shows one of the finished splice joint.

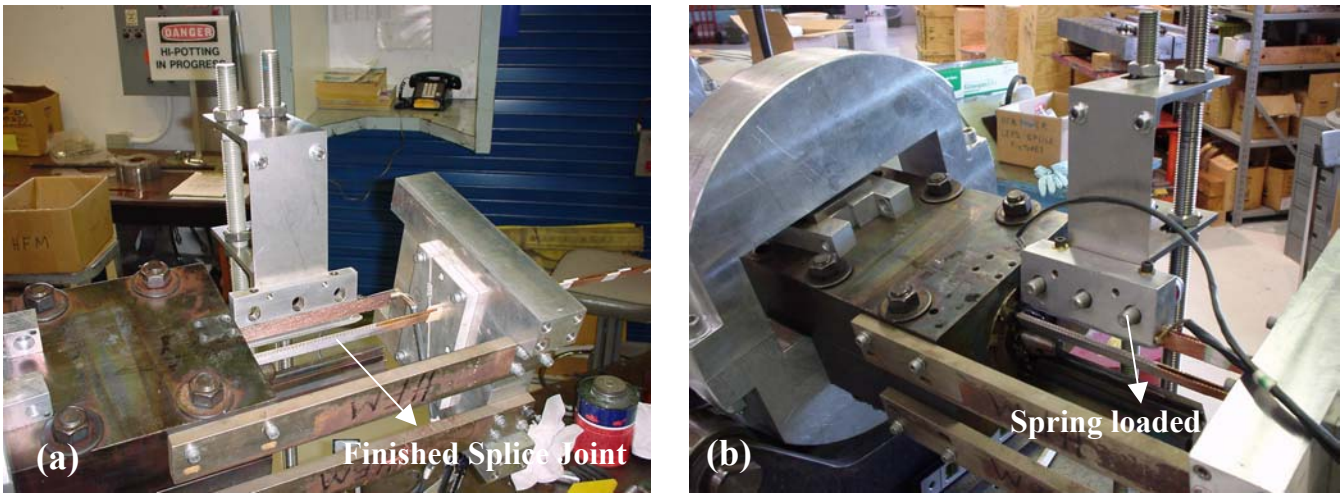

Fig. 7: *Set up for splicing operation.*

6.0 EPOXY IMPREGNATION

The reacted coil was transferred from the reaction fixture to the impregnation fixture using rollover assembly. The coil was inspected during this transfer and no tin-leakage was observed. One voltage tap per outer layer of the each half-coil near the inner to outer layer transition was also installed during the transfer. Thin stainless steel strip was soldered to the cable and 1 mil thick Kapton layer was installed on top of the voltage tap. Fig. 8 shows the coil assembly with one of voltage taps.

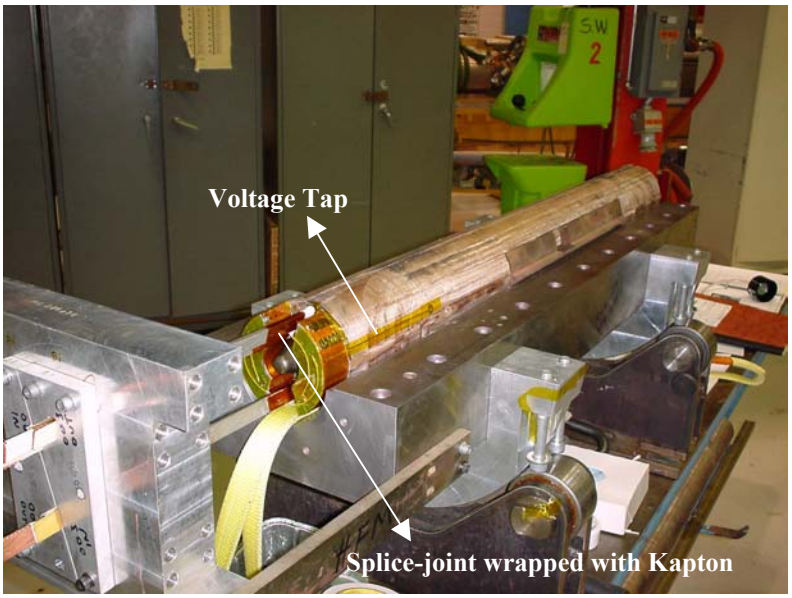

Fig. 8: *Outer layer showing the voltage tap.*

Fig. 9: *Epoxy impregnated coil assembly.*

To avoid any contact between the epoxy and the bare cable, each splice joint was wrapped with Kapton (also shown in Fig. 8). Further to reduce the amount of epoxy, the gap between the splice support fixtures was filled with fiberglass insulation. The impregnation procedure followed was similar to that of HFDA-02. The one difference between the two was that the intake of epoxy was never stopped in HFDA-03 as the flow rate was well regulated by adjusting the pressure. The whole process took about 5 hrs. Fig. 9 shows the impregnated coil assembly.

Electrical measurements (L, Q, and R) were performed on the impregnated coil assembly. Table 4 shows the data. For comparison measurements taken before reaction were also included in the table. The resistance of the coil assembly after reaction increased by about 70%. The Q decreased by the same amount as the inductance of the coil remained constant before and after reaction. Most importantly the two coils have similar values, which indicate that there are no turn-to-turn shorts. Note that L and Q are measured at 1 kHz. Additional electrical measurements are given in Table 5.

Parameter	Before Reaction		After Reaction and Impregnation	
	HFDAH-05	HFDAH-06	HFDAH-05	HFDAH-06
Resistance, mΩ	59.27	58.26	102.05	101.04
Inductance, μH	245.86	245.70	217.78	217.43
Quality Factor	6.94	7.17	3.63	3.64

Table 4: *Electrical measurements of coil after reaction and impregnation.*

Coil	Resistance, mΩ	Inductance, μH		Quality Factor	
		At 1.0 kHz	At 20 Hz	At 1.0 kHz	At 20 Hz
HFDAH-005 (inner layer)	45.30	75.05	--	0.95	--
HFDAH-005 (outer layer)	58.86	119.05	--	1.35	--
HFDAH-006 (inner layer)	44.37	75.60	--	0.85	--
HFDAH-006 (outer layer)	56.20	119.74	--	1.21	--
HFDAH-005	102.05	217.78	281.22	3.63	0.29
HFDAH-006	101.04	217.43	278.10	3.64	0.30
TOTAL	205.00	657.94	846.81	4.13	0.47

Table 5: *Additional Electrical measurements on the half-coils after reaction and impregnation.*

Hi-Pot tests up to 1 kV were also performed on the impregnated coil assembly to check current leakage between coil to ground, coil to heaters and heaters to ground. While the current leakage between coil to ground and heater to ground was less than 0.04 μA at 1 kV, the leakage between coil to heaters exceeded 0.5 μA at 600 V. It's believed that the conductive flux used to facilitate soldering on to the strip-heaters might have caused this leakage. Since the maximum voltage applied at the VMTF is less than 500 V, the fabrication of the magnet was continued. However, we are presently looking into ways to avoid such a leakage in future magnets.

7.0 INSTRUMENTATION

One outer pole piece on each half-coil was mold released before epoxy impregnation so that they can be removed after impregnation. Two outer pole pieces were modified to accept capacitance gauges and were placed at these locations. Resistive gauges were mounted on the circumferential grooves made on the aluminum spacers. Fig 10 shows the layout of gauges in the magnet cross-section. The capacitance gauges measure the azimuthal stress in the outer layer of the half-coils while the resistive gauges measure the azimuthal stress in the aluminum spacers.

In order to estimate the stress distribution near the splice joint, the last Aluminum spacer both on the top and bottom side were also instrumented with resistive gauges.

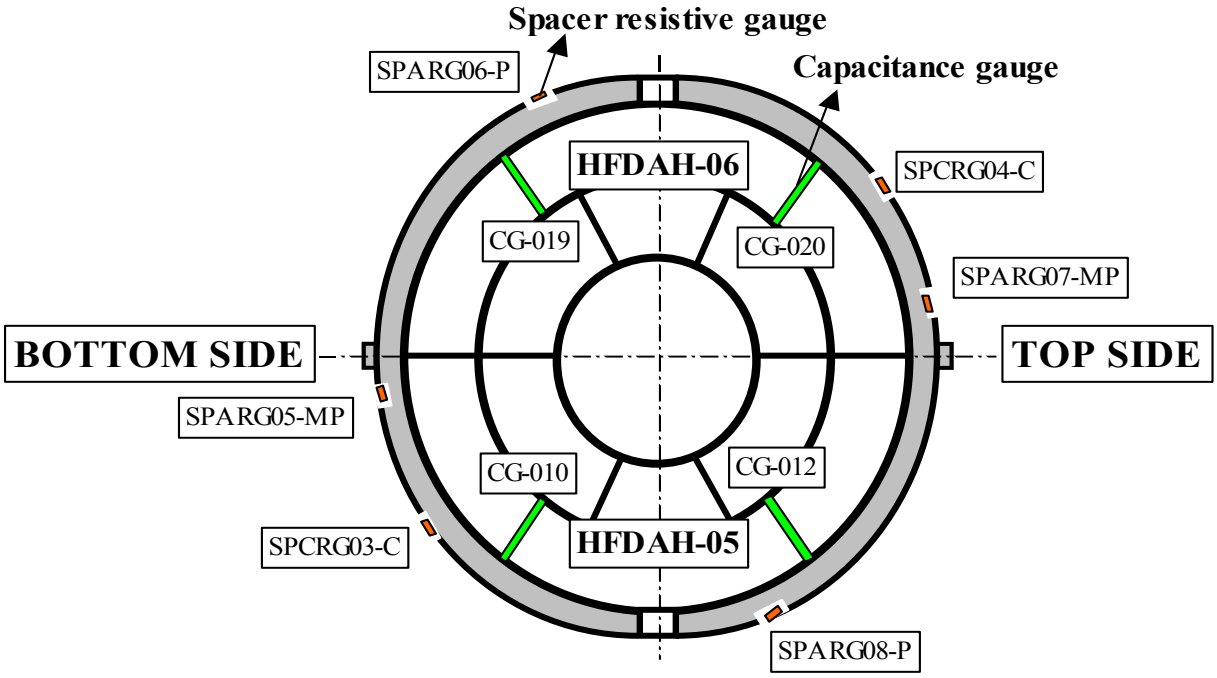

Fig. 10: *Layout of gauges in the magnet cross-section.*

8.0 YOKING

The impregnated coil assembly was measured using CORDAX machine for determining the geometry of the coil assembly. The outer radius of the impregnated coil was found to be 50 μm under the nominal size. Further, similar to HFDA-02, the outer pole pieces had shifted by 50 μm to the left side (in the Fig. 10) with respect to the center of the coil. To account for these deviations and still maintain symmetry, 100 μm brass shim was placed between the spacer and the outer pole piece extension on the left side with 100 μm radial Kapton shim on the coil assembly.

The pump pressure was increased in 1000 Psi increments and the gauge readings were recorded. During the first loading we still noticed asymmetry in loading between topside and bottom side of the coil

assembly (see Fig. 11) with the bottom side of the coil about 15 MPa less than the ANSYS calculations. Note that top and bottom side represents half of each coil. Fig. 12 shows the evolution of azimuthal stress in the spacers with pump pressure. The magnet was disassembled and the imprints on the Kapton layer showed that the outer pole pieces were not compressed to the same extent as the rest of the coil assembly. Note that the ground insulation did not extend over the outer pole pieces and this has caused a step. Therefore, 100 μm thick Kapton shim with adhesive was glued radially on the outer pole pieces. The coil assembled was then yoked and compressed in 1000 Psi increments. This time the coil stress was very high compared to the expected values (also shown in Fig. 10). However, when the magnet was disassembled the Kapton insulation had uniform imprint. So the radial shim on the outer pole pieces were kept and the radial insulation on the entire coil assembly was reduced from 100 μm to 50 μm. The coil assembly was again yoked and re-tested. Figs. 13 and 14 shows the stress evolution in the last iteration for the coil and spacers respectively. The bottom and topside of the each half-coil is within 5-10 MPa range. Also shown in Fig. 14 is the azimuthal stress distribution in the spacer near the LE. The stress distribution in the mid-plane of the pole is consistent with that of the straight section, however near the pole region it has much higher stress. Note that during the entire loading operation, 40 mil thick stainless steel shims were placed near the LE and RE so as not to over compress.

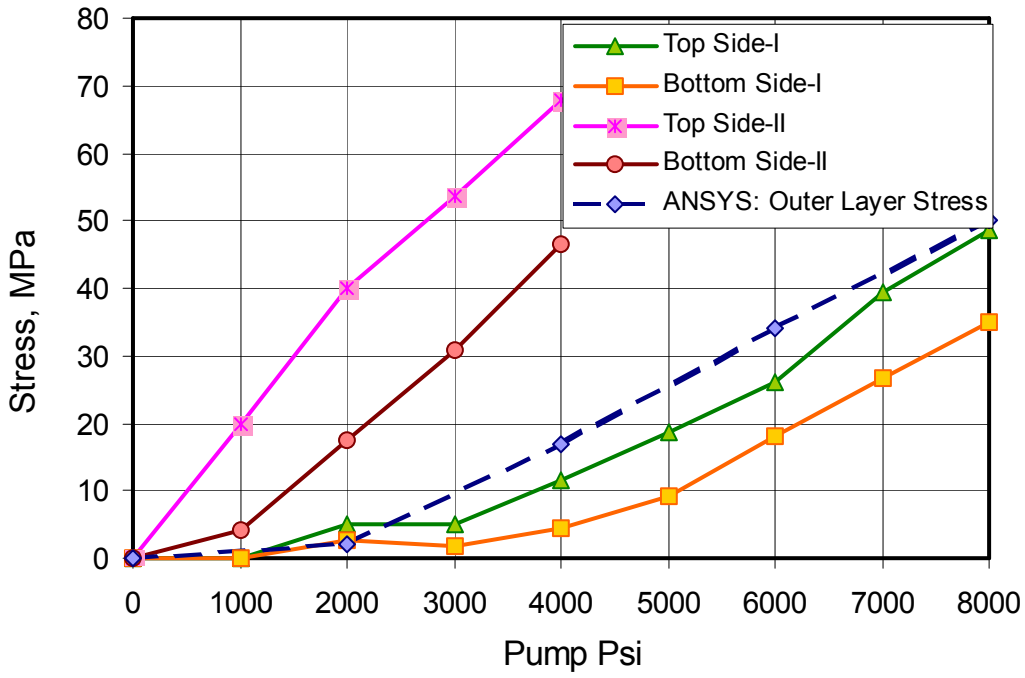

Fig. 11: *Evolution of azimuthal stress in the outer layer of coil with pump pressure. I and II represent first and second iterations.*

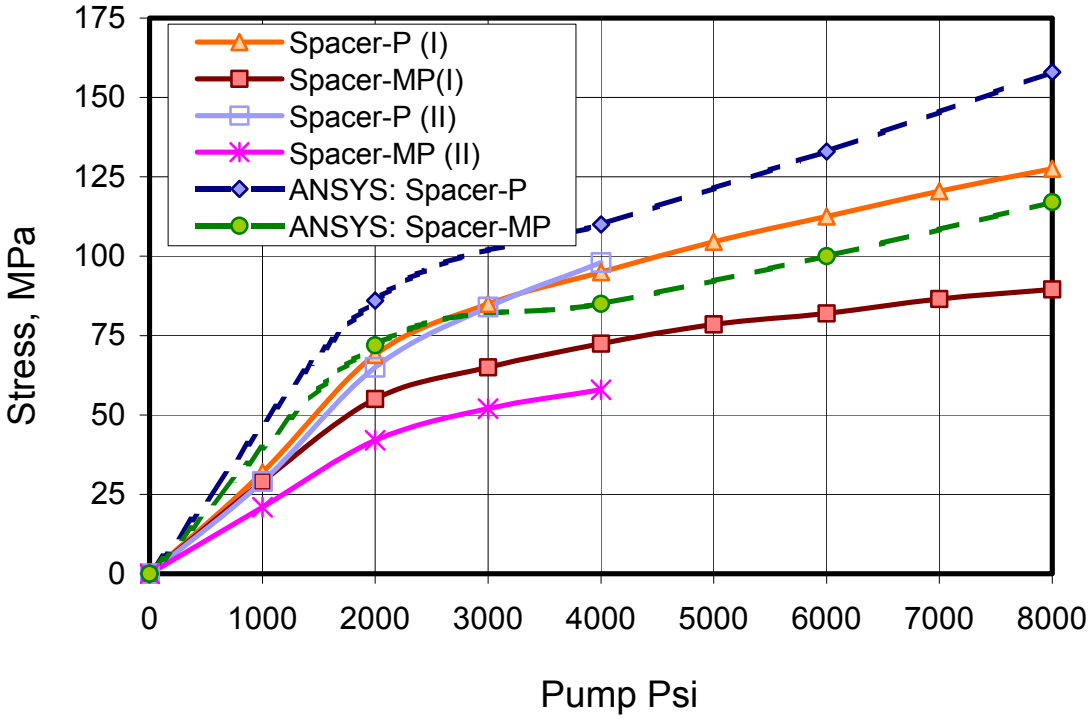

Fig. 12: *Evolution of the azimuthal stress in the spacer. Note that 'P' represent pole and 'MP' represent mid-plane. Each experimental data represent average between two gauge readings, one on topside spacer and the other on bottom side spacer.*

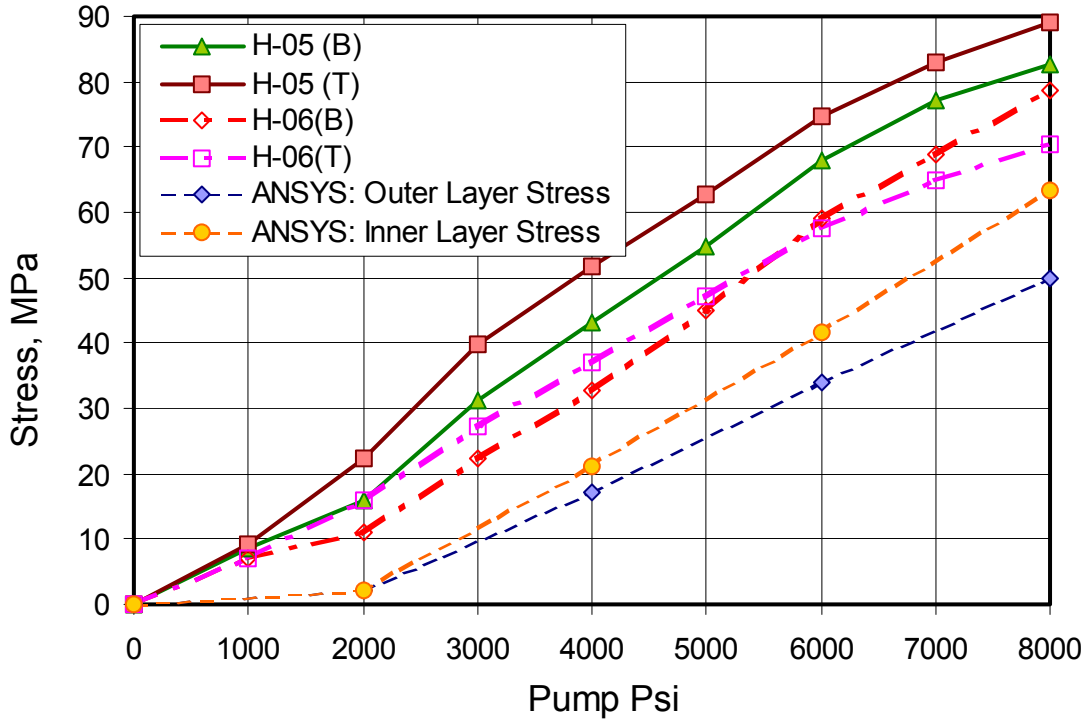

Fig. 13: *Evolution of azimuthal stress in the outer layer of the coil with pressure for the final iteration.*

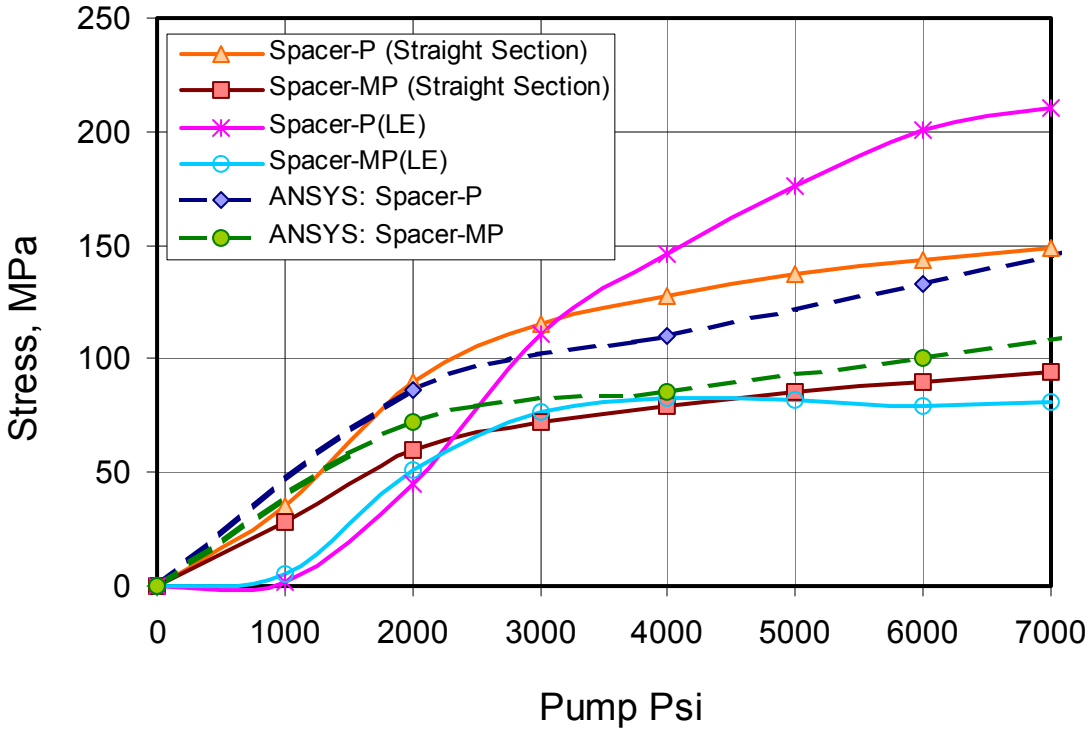

Fig. 14: *Evolution of the azimuthal stress in the spacer for the final iteration.*

	UNDER PRESS MPa	DURING CLAMPING MPa	AFTER SPRING BACK MPa	AFTER WELDING SKIN MPa
HFDA-03				
COIL OUTER LAYER	76	80	24	54
SPACER-POLE	153	157	97	120
SPACER-MIDPLANE	92	96	83	90
SKIN				~ 225
ANSYS				
COIL OUTER LAYER	50		20	60
SPACER-POLE	160		108	165
SPACER-MIDPLANE	118		84	117
SKIN				216

Table 6: *Summary of data collected during yoking and skinning.*

At 8000 pump Psi, the gap between the yoke halves was close to the nominal value and the clamps were inserted using a separate set of pusher blocks. Two clamps, one on each side were inserted

simultaneously starting from the middle of the magnet. Note that during the entire operation the coil resistance was monitored to make sure we do not have any turn-to-turn shorts. Table 6 gives the summary of the data collected during yoking. The ANSYS data is also given in the table. The azimuthal stress in the coil outer layer pole region after springback is about 24 MPa.

9.0 SKINNING AND END-PLATE INSTALLATION

The next step in the magnet assembly is to weld the two skin halves on to the yoked assembly. First the skin alignment keys were inserted into the grooves provided in the aluminum clamps. The whole assembly is then gently placed in the lower half of the skin that is already installed in the welding press. The upper half of the skin is then installed on the magnet. The two skin halves were compressed at 600 pump Psi during welding operation. After each weld pass, the distance between the top and bottom pushers was measured to compute weld shrinkage. Simultaneously the gauge readings were recorded to monitor the increase in coil stress with weld shrinkage. Fig. 15 shows the evolution of stress in the coil with the weld shrinkage. The stress in the skin was also monitored during welding operation. The mean azimuthal stress in the skin exceeded the yield limit, which is about 225 MPa.

After welding the ends of the skins were cut to the right dimensions. Seven gauges were installed along the length of the skin to measure the longitudinal stress in the skin during excitation. The end plates were then welded on both lead and return ends to provide axial support to the coils. Finally the twist along the length of the magnet was measured using twist-measuring device. Fig. 16 shows the variation of the twist along the length of the magnet.

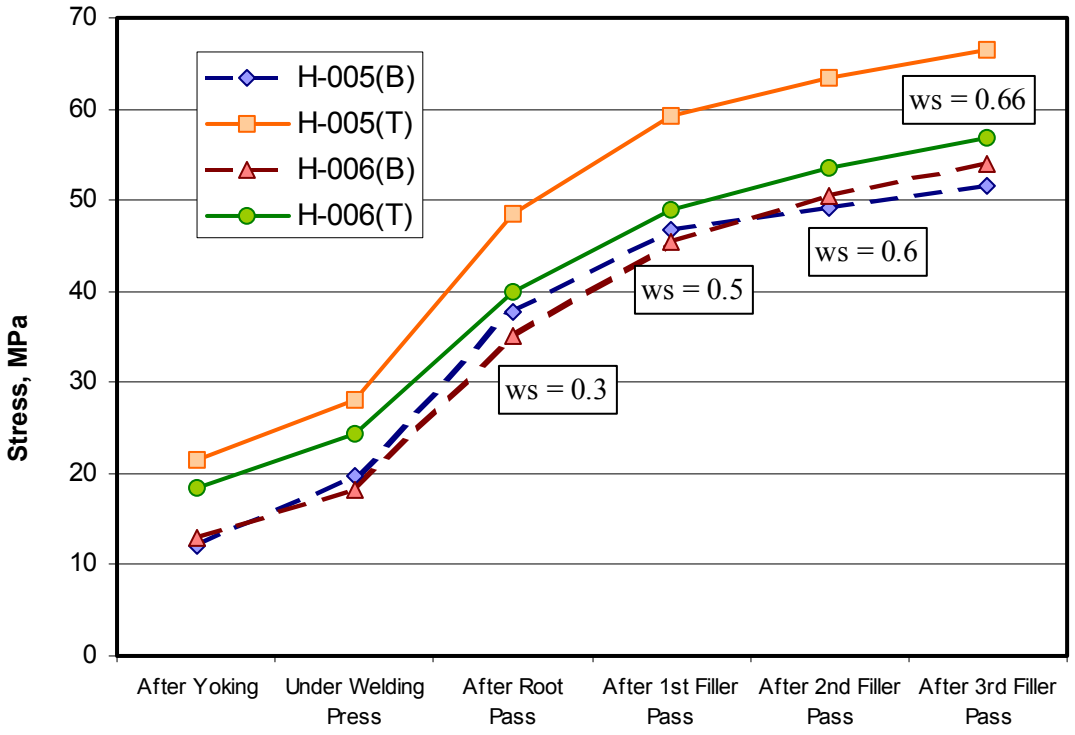

Fig. 15: *Evolution of coil stress with weld shrinkage. Note that B and T represent bottom and top side.*

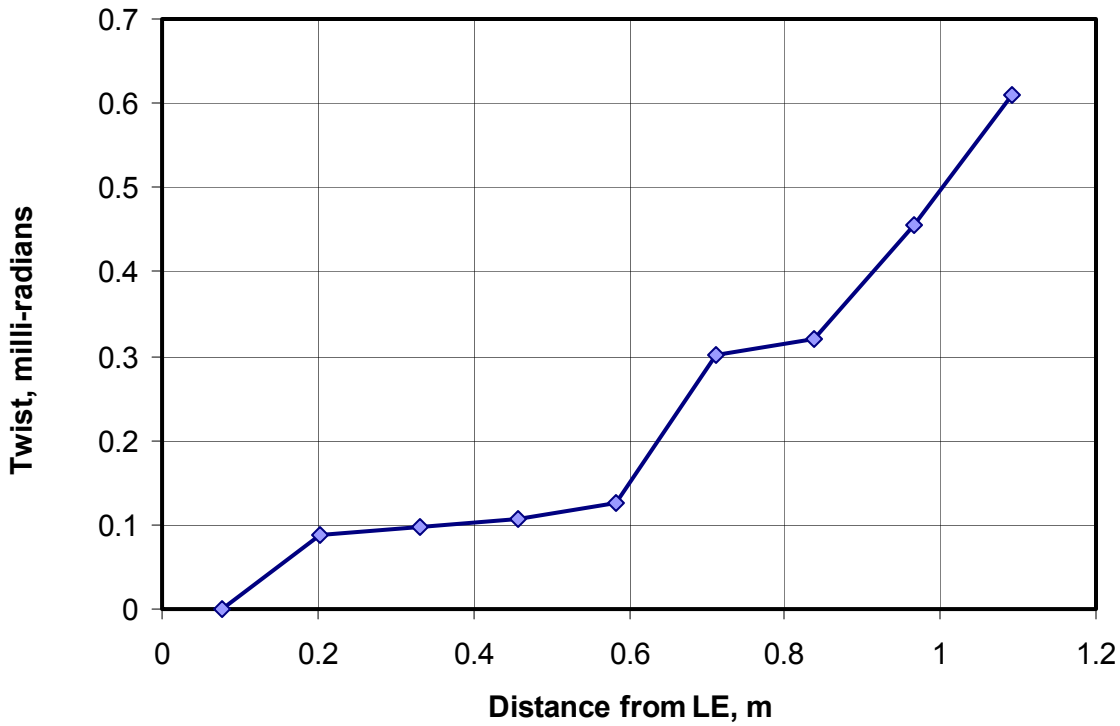

Fig. 16: *Variation of twist along the length of the magnet.*

10.0 FINAL ASSEMBLY

Once the end plates were welded, the bullets were installed on both LE and RE. Four bullets per end were torqued until each bullet sees 500 lbs of force. Note that the bullets were installed with strain gauges and were calibrated both warm and cold.

The last mechanical assembly involved performing the half-coil splices. The outer layer leads from both the half-coils were spliced together and captured in a G-10 box. The inner layer leads were used as power leads for the magnet. The half-coil splice assembly was achieved without fixing the leads using "green putty" to the G-10 spacers. This would enable the leads to move under Lorentz forces if necessary

Several voltage taps were installed on the lead cables before installing the splice box assembly as per drawing MB-411080. All the wires were finally terminated into hypertronic connectors to be hooked up in VMTF.

Electrical measurements were performed on the magnet just before shipping it to the VMTF. Table 7 summarizes these measurements.

	Resistance mΩ	Inductance, mH		Quality Factor	
		At 1 kHz	At 20 Hz	At 1 kHz	At 20 Hz
HFDAH-05	98.85	0.126	0.355	1.30	0.20
HFDAH-06	98.77	0.128	0.347	1.32	0.20
Total Magnet	197.41	0.344	1.102	1.42	0.59

Table 7: *Electrical measurements on the half-coils and the total magnet.*

The coil bore diameter was measured at different stages of the magnet fabrication. Table 8 summarizes the data. Note that the nominal bore diameter is 43.0 mm.

	RE		LE	
	@ 75mm from the end	@ End-saddles	@ 75mm from the end	@ end-saddles
After Epoxy Impregnation	43.116	43.129	43.383	42.799
After Yoking/Clamping	42.964	42.926	--	--
After Welding Skin	42.926	42.901	--	--

Table 8: *Coil bore diameter measurements at various stages of the magnet fabrication.*

11.0 SUMMARY

The third shell-type Nb_3Sn high field dipole magnet was delivered to VMTF for testing on August 27, 2001.

Several issues such as asymmetry in the stress distribution between top and bottom side of the coil assembly, strand damage during splicing, half-coil splice assembly without using green-putty have been addressed in this magnet. However the large amount of epoxy still surround near the beginning of the splice joint. Note that the splice joint itself is covered with Kapton layer. A new splice support has been designed for the next magnet to avoid this excessive epoxy presence near the Nb_3Sn cable.